Research Article

Sciences of Pharmacy

Green-Synthesized Silver Nanoparticles Using *Erythrina subumbrans* Leaf Extract: Optimization and Antibacterial Activity

Indri Maharini, Karen Putri Utami, Lilis Rachmawati, Fitrianingsih Fitrianingsih, Puspa Dwi Pratiwi

[The author informations are in the declarations section. This article is published by ETFLIN in Sciences of Pharmacy, Volume 5, Issue 2, 2026, Page 112-122. DOI: 10.58920/sciphar0502580]

Received: 01 February 2026
Revised: 01 March 2026
Accepted: 07 April 2026
Published: 21 April 2026

Editor: Garnadi Jafar

This article is licensed under a Creative Commons Attribution 4.0 International License. © The author(s) (2025).

Keywords: Erythrina subumbrans, silver nanoparticles, green synthesis, Box–Behnken design, antibacterial activity, Propionibacterium acnes.

Abstract: The high prevalence of acne and increasing antibiotic resistance necessitate the development of sustainable antimicrobial agents. This study investigated the green synthesis of silver nanoparticles (AgNPs) using *Erythrina subumbrans* (Hassk.) Merr. leaf extract as a natural bioreductant and stabilizer. The primary objective was to optimize the synthesis process and evaluate the antibacterial efficacy of the resulting nanoparticles specifically against *Propionibacterium acnes*. Physicochemical and structural characterization were performed using spectroscopic and microscopic techniques to confirm the formation and stability of the nanoparticles. The results successfully demonstrated the synthesis of crystalline, nanoscale AgNPs with plant-derived functional groups facilitating their stabilization. Analytical data indicated a relatively uniform particle size distribution, spherical morphology, and favorable surface characteristics, suggesting high suitability for biomedical integration. Significantly, the synthesized AgNPs exhibited potent antibacterial activity against *P. acnes*. The underlying mechanism of action is attributed to the disruption of bacterial cell membranes, induction of intracellular reactive oxygen species, and subsequent interference with vital cellular functions. Utilizing *E. subumbrans* extract offers an eco-friendly, cost-effective, and sustainable alternative to conventional chemical synthesis, reducing the reliance on toxic reagents. These findings highlight the significant potential of plant-mediated AgNPs as innovative antimicrobial agents for dermatological applications. This research provides a robust foundation for the advancement of nanotechnology-based topical treatments. Consequently, further investigation into pharmaceutical formulation development, comprehensive safety assessments, and clinical efficacy trials is highly recommended to establish *E. subumbrans*-mediated silver nanoparticles as viable therapeutic solutions for managing acne and other skin-related infections in the future.

Introduction

Indonesia is rich in medicinal plants with long-standing traditional uses, one of which is *Erythrina subumbrans* (Hassk.) Merr., commonly known as dadap serep. This plant grows widely in tropical and subtropical regions, including Indonesia, the Philippines, Thailand, and Malaysia (1). In traditional medicine, the leaves and stem bark of *E. subumbrans* are frequently utilized. The leaves have been empirically used to treat fever, postpartum fever, inflammation, bleeding, abdominal pain, and to promote lactation, while the stem bark is traditionally used as an expectorant (2). Pharmacological studies have reported that *E. subumbrans* leaves exhibit antipyretic, anti-inflammatory, antioxidant, and antibacterial activities (3). These biological activities are attributed to the presence of various secondary metabolites, including phenolics, tannins, alkaloids, flavonoids, saponins, and steroids (4). Previous studies demonstrated that extracts of *E. subumbrans* showed antibacterial activity against g-positive bacteria, with minimum inhibitory concentrations ranging from 2 to 4 µg/mL (5).

Beyond their antibacterial properties, secondary metabolites in *E. subumbrans* leaves also possess substantial reducing and stabilizing capabilities, making them promising natural bioreductants for the green

synthesis of silver nanoparticles. Compounds such as flavonoids, phenolics, alkaloids, and tannins are known to facilitate the reduction of silver ions (Ag^+) to elemental silver (Ag^0) while simultaneously stabilizing the formed nanoparticles (6, 7). Several studies have successfully employed plant extracts as bioreductants in silver nanoparticle synthesis, including extracts from *Areca catechu* L. (8), *Musa paradisiaca* (9), *Imperata cylindrica* L. (10), *Dendrobium crumenatum* (6), and *E. subumbrans* stem bark (4), supporting the feasibility of plant-mediated nanoparticle synthesis. The stem of *E. subumbrans* has been previously reported to contain flavonoids, saponins, isoflavonoids, alkaloids, and lectins that function as effective bioreductants in nanosilver biosynthesis. Earlier studies demonstrated that variation in stem extract concentration significantly influenced AgNP formation, yielding SPR peaks at 429–436 nm and particle sizes ranging from 66.13 to 75.96 nm with PDI values below 0.5, indicating uniform nanoparticle distribution and optimal stability at a 1: 1 extract-to-$AgNO_3$ ratio (3). Despite these findings, existing research has been exclusively limited to the stem part of *E. subumbrans*, leaving the bioreductive potential of its leaves entirely unexplored.

Nanoparticles are materials with particle sizes ranging from 1 to 100 nm and exhibit unique physicochemical properties (11). Among various metal and metal oxide nanoparticles, silver nanoparticles (AgNPs) have attracted considerable attention due to their superior antibacterial activity, even at low concentrations, compared to zinc oxide and gold nanoparticles (12–20). The strong antibacterial efficacy of AgNPs makes them promising candidates for addressing the growing concern of antibiotic resistance. Silver nanoparticles can be synthesized through physical, chemical, and biological methods. Although physical and chemical processes can produce nanoparticles rapidly, they often require high energy input, toxic chemicals, and generate hazardous by-products. In contrast, green synthesis using biological resources, particularly plant extracts, offers an environmentally friendly, cost-effective, and non-toxic alternative. In this approach, natural bioreductants facilitate the reduction of Ag^+ ions through electron transfer mechanisms and functional group transformations (21–23).

Synthesis parameters, such as $AgNO_3$ concentration, temperature, and incubation time, strongly influence the efficiency and characteristics of green-synthesized silver nanoparticles (24). Therefore, optimization of these parameters is essential to obtain nanoparticles with desirable physicochemical properties and enhanced antibacterial activity. It is proposed that the aqueous extract of *E. subumbrans* leaves functions as a natural bioreductant and capping agent during green silver nanoparticle synthesis, thereby generating nanoparticles with optimized physicochemical attributes and improved stability. This dual role is expected to influence particle size, morphology, and surface characteristics, which are critical factors affecting biological activity. Based on these considerations, this study aimed to optimize the green synthesis of silver nanoparticles using *E. subumbrans* leaf extract as a natural bioreductant through a Box–Behnken experimental design implemented in Design-Expert® software. The optimization focused on key synthesis parameters to achieve maximum efficiency and reproducibility of nanoparticle formation. Furthermore, the antibacterial activity of the optimized silver nanoparticles against *Propionibacterium acnes* was systematically evaluated to determine their potential as alternative antimicrobial agents. The results of this study are expected to contribute to the development of eco-friendly and sustainable antibacterial nanomaterials derived from indigenous medicinal plants, as well as provide a scientific basis for their application in pharmaceutical and dermatological formulations.

Methodology

Equipment

The instruments used in this study were an analytical balance (Pioneer PX Series, OHAUS, Germany/USA), a hot plate magnetic stirrer (DLAB MSH280-Pro, China), an autoclave, an incubator (Memmert, Germany), a laminar air flow cabinet (Biobase, China), a UV–visible spectrophotometer (Thermo Scientific Genesys 10S, USA), a Fourier transform infrared (FTIR) spectrometer (Bruker Alpha II, Germany), a particle size analyzer (SZ-100, HORIBA Scientific, Japan), an X-ray diffractometer (Bruker D8 Advance, USA), and a scanning electron microscope equipped with energy-dispersive X-ray spectroscopy (SEM-EDX; Carl Zeiss EVO 10, Germany).

Materials

The materials used in this study were deionized water (OneMed®), *E. subumbrans* (Hassk.) Merr. leaves, silver nitrate ($AgNO_3$; Merck®, Germany), and the test bacterium *Propionibacterium acnes*. The reagents employed included Mayer's reagent, Dragendorff's reagent, hydrochloric acid, sulfuric acid, Liebermann–Burchard reagent, 10% sodium hydroxide solution, chloroform, and ferric chloride (all supplied by PT Kimia Jaya Labora, Indonesia).

Methods

Preparation of *Erythrina subumbrans* Leaf Extract

Leaves of *E. subumbrans* (Hassk.) Merr. were collected from Mendalo Indah Village, Muaro Jambi Regency, Jambi Province, Indonesia, and taxonomically identified at Universitas Padjadjaran, Indonesia, as confirmed by a certificate of determination (No. 56/HB/12/2025). The leaves were cleaned by wet sorting, washed briefly with running water, cut into uniform pieces, and dried at 60 °C for 48 h. The dried material was powdered, sieved through a 60-mesh sieve, and used for extraction. Extraction was performed by the infusion method by heating 0.75 g of leaf powder in 100 mL of deionized water (0.75% w/v) at approximately 90 °C for 15 min with occasional stirring. The mixture was cooled, filtered, and the obtained filtrate was used directly for silver nanoparticle synthesis (4).

Phytochemical screening

Phytochemical screening was conducted to qualitatively determine the presence of flavonoids, saponins, alkaloids, tannins, phenolics, and steroids/triterpenoids in the extract using standard procedures. The presence of flavonoids was confirmed through the Shinoda test, indicated by the formation of a pink to reddish coloration after the addition of magnesium and hydrochloric acid. Saponins were identified based on the formation of stable foam following

vigorous shaking and acidification. Alkaloids were detected using Dragendorff's and Mayer's reagents, which yielded orange and cream precipitates, respectively. Tannins and phenolic compounds were verified using the ferric chloride test, characterized by the appearance of dark blue, green, or black coloration. Steroids and triterpenoids were assessed using the Liebermann–Burchard reaction, indicated by the development of green or bluish coloration. These qualitative analyses provide preliminary evidence of the presence of bioactive compounds that may contribute to the reduction and stabilization processes during nanoparticle synthesis (2).

Optimization of Silver Nanoparticle Synthesis

Optimization of silver nanoparticle synthesis was conducted using response surface methodology with a Box–Behnken design in Design-Expert® version 13 by varying $AgNO_3$ concentration, temperature, and incubation time. Each factor was evaluated at two levels (low and high), as shown in **Table 1**, with the experimental design comprising 17 runs (**Table 2**). Silver nanoparticles were synthesized by mixing *E. subumbrans* leaf extract and $AgNO_3$ solution at a 1: 1 ratio and heating under the specified conditions. Nanoparticle formation was indicated by a color change from yellow to brown. At the same time, optical responses, including absorbance, surface plasmon resonance (SPR) peak, and transmittance, were analyzed using UV–Visible spectroscopy (200–800 nm) to determine the optimal synthesis conditions. Optimum synthesis conditions were determined using response surface methodology with a Box–Behnken design in Design-Expert® version 13, optimizing response goals within defined limits; desirability values approaching 1 indicated optimal silver nanoparticle synthesis.

Characterization of Optimized Silver Nanoparticles

The optimized silver nanoparticles were characterized for their optical properties, size distribution, surface charge, functional groups, morphology, and crystalline structure. Absorbance, surface plasmon resonance (SPR), and transmittance were analyzed by UV–Visible spectroscopy over 200–800 nm, with transmittance measured at 650 nm. Particle size, polydispersity index (PDI), and zeta potential were determined using a particle size analyzer (PSA). Functional groups involved in nanoparticle formation were identified by Fourier transform infrared (FTIR) spectroscopy in the range of 400–4000 cm^{-1} after freeze-drying. Prior to this step, the nanoparticle suspension was centrifuged at 5000 rpm for 30 min, the supernatant was removed, and the resulting pellet was washed with

Table 1. Experimental parameters and their coded levels for silver nanoparticles synthesis optimization.

Parameter	Coded Level –1	Coded Level +1
AgNO3 Concentration (mM)	1	3
Incubation Time (h)	1	3
Temperature (°C)	50	90

Table 2. Box–Behnken experimental design and response values for the optimization of green synthesis of silver nanoparticles using *E. subumbrans* leaf extract.

Run	$AgNO_3$ Concentration (mM)	Incubation Time (h)	Temperature (°C)	Absorbance	SPR (nm)	Transmittance (%)
1	1	3	70	0.95549	422	79.2
2	3	2	90	2.54913	424	62.1
3	2	1	90	2.20896	424	69.7
4	2	3	90	2.50004	430	65.2
5	2	2	70	1.75821	422	70.1
6	3	1	70	1.53181	422	73.3
7	3	2	50	3.18294	418	54.7
8	2	2	70	2.33894	422	62.6
9	1	2	90	2.67786	420	68.6
10	2	2	70	2.02441	422	69.0
11	2	1	50	3.31106	422	54.1
12	2	2	70	2.15886	422	68.0
13	1	2	50	1.88862	422	64.5
14	1	1	70	1.26003	420	69.8
15	2	3	50	3.00805	418	61.0
16	2	2	70	2.74586	418	48.6
17	3	3	70	2.95405	424	36.0

deionized water to eliminate residual impurities before analysis. Particle morphology was examined using scanning electron microscopy (SEM), while crystalline structure was analyzed by X-ray diffraction (XRD) using Cu-Kα radiation.

Antibacterial Activity Assay

Antibacterial activity against *Propionibacterium acnes* was evaluated using the Kirby-Bauer disc diffusion method. A bacterial suspension was precisely adjusted to a 0.5 McFarland standard and uniformly inoculated onto sterile nutrient agar plates to create a confluent growth. Sterile 6 mm paper discs were then impregnated with 20 µL of the synthesized silver nanoparticles. For a comprehensive comparative analysis, $AgNO_3$ solution and Mediklin® Gel 1% were employed as negative and positive controls, respectively, while the pure leaf extract was tested separately to determine its baseline activity. After incubation at 37 °C for 24 h under appropriate conditions, the resulting inhibition zones were measured using a digital caliper. All assays were conducted in triplicate to ensure statistical reliability and results were expressed as mean diameters.

Results and Discussion

Phytochemical screening

Phytochemical screening was conducted to identify secondary metabolites with potential roles in bioreduction during silver nanoparticle synthesis. As shown in **Table 3**, the aqueous extract of *E. subumbrans* leaves tested positive for flavonoids, tannins, and phenolic compounds, while saponins, alkaloids, and steroids/triterpenoids were not detected. An orange coloration in the Shinoda test indicated the presence of flavonoids. In contrast, positive reactions for tannins and phenolics were confirmed by the formation of dark brown to black color with ferric chloride, suggesting complex formation between Fe^{3+} ions and phenolic hydroxyl groups. The absence of stable foam, precipitate formation, or characteristic color changes

Table 3. Phytochemical screening results of *E. subumbrans* (Hassk.) Merr. leaf extract.

Phytochemical Test	Reagent	Result	Observation
Flavonoids	Concentrated HCl + Mg powder	+	Formation of orange coloration
Saponins	2 N HCl	–	No stable foam formation
Alkaloids	Mayer's reagent	–	No yellowish-white precipitate formation
Tannins	3% $FeCl_3$	+	Formation of dark brown coloration
Phenolics	5% $FeCl_3$	+	Formation of dark brown coloration
Steroids/Triterpenoids	Liebermann–Burchard reagent	–	No red, orange, or blue coloration

Table 4. ANOVA of the quadratic model for Ag-NP synthesis optimization using response surface analysis.

Source	Sum of Squares	df	Mean Square	F-value	p-value	Significance
Model	709.67	14	50.69	3.36	0.0209	significant
A-Tem. (C)	280.33	1	280.33	18.59	0.0010	
B-Incubation Period	0.3333	1	0.3333	0.0221	0.8843	
C-AgNO3 Conc. (mM)	48.00	1	48.00	3.18	0.0997	
D-Extract Volume (mL)	5.33	1	5.33	0.3536	0.5631	
AB	1.00	1	1.00	0.0663	0.8012	
AC	169.00	1	169.00	11.20	0.0058	
AD	1.0000	1	1.0000	0.0663	0.8012	
BC	1.0000	1	1.0000	0.0663	0.8012	
BD	121.00	1	121.00	8.02	0.0151	
CD	16.00	1	16.00	1.06	0.3234	
A^2	33.33	1	33.33	2.21	0.1629	
B^2	5.33	1	5.33	0.3536	0.5631	
C^2	0.3333	1	0.3333	0.0221	0.8843	
D^2	16.33	1	16.33	1.08	0.3186	
Residual	181.00	12	15.08			
Lack of Fit	149.00	10	14.90	0.9313	0.6220	not significant
Pure Error	32.00	2	16.00	-	-	
Cor Total	890.67	26	-	-	-	

evidenced negative results for saponins, alkaloids, and steroids/triterpenoids. These findings are partially consistent with previous studies (1), with variations likely attributed to differences in extraction methods, solvents, and extract concentrations, which may influence metabolite detectability. The phytochemical analysis was limited to qualitative identification without quantitative measurement of metabolite levels. This restricts detailed mechanistic interpretation of their role in Ag-NP synthesis, highlighting the need for quantitative profiling in future studies.

Optimization of Silver Nanoparticle Synthesis

Silver nanoparticle formation was indicated by a color

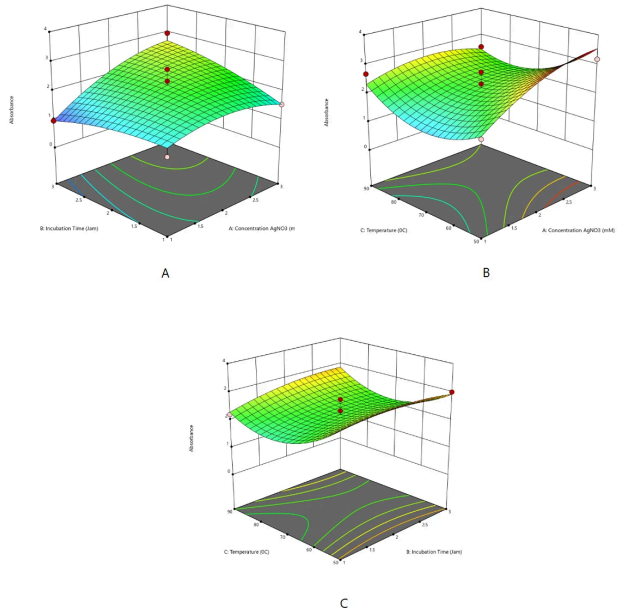

Figure 1. Surface plots illustrating the combined effects of (A) concentration of AgNO3 and incubation time, (B) concentration of AgNO3 and Temperature, and (C) incubation time and temperature on Ag-NP synthesis efficiency. The vertical axis corresponds to absorbance, reflecting the efficiency of silver nanoparticle formation.

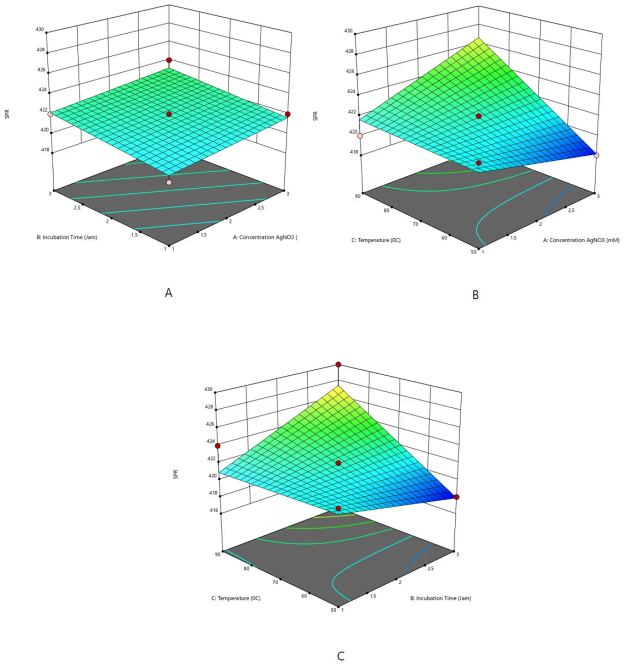

Figure 2. Surface plots illustrating the combined effects of (A) concentration of AgNO3 and incubation time, (B) concentration of AgNO3 and Temperature, and (C) incubation time and temperature on Ag-NP synthesis efficiency. The vertical axis denotes the SPR value, representing the efficiency of silver nanoparticle synthesis.

change from pale yellow to reddish-brown, confirming the reduction of Ag^{+} to Ag^{0}. Increasing $AgNO_3$ concentration, heating temperature, and heating time resulted in a darker solution color, indicating greater nanoparticle formation. Synthesis optimization was performed using response surface methodology with a Box–Behnken design, evaluating absorbance, surface plasmon resonance (SPR) wavelength, and transmittance. The absorbance values ranged from 0.96 to 3.31, with SPR peaks observed at 418–430 nm, consistent with the characteristic SPR region of silver nanoparticles (**Table 2**). Transmittance values (36–81.7%) showed an inverse relationship with absorbance, in accordance with the Beer–Lambert law, indicating increased nanoparticle formation at higher absorbance levels.

The absorbance response was statistically analyzed using ANOVA for the polynomial response surface model (**Table 4**). The model was statistically significant (F = 3.36; p = 0.0209), and the non-significant lack-of-fit indicates good agreement between the predicted and experimental

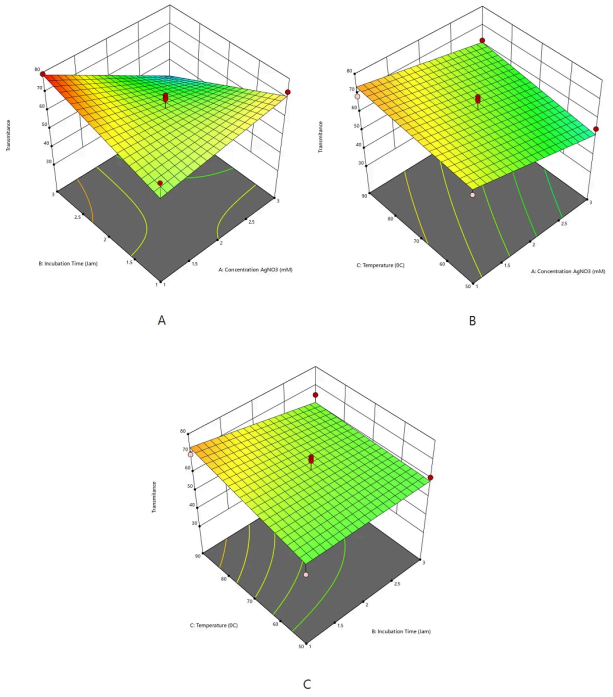

Figure 3. Surface plots illustrating the combined effects of (A) concentration of AgNO3 and incubation time, (B) concentration of AgNO3 and Temperature, and (C) incubation time and temperature on Ag-NP synthesis efficiency. The vertical axis denotes transmittance, reflecting the efficiency of AgNP synthesis.

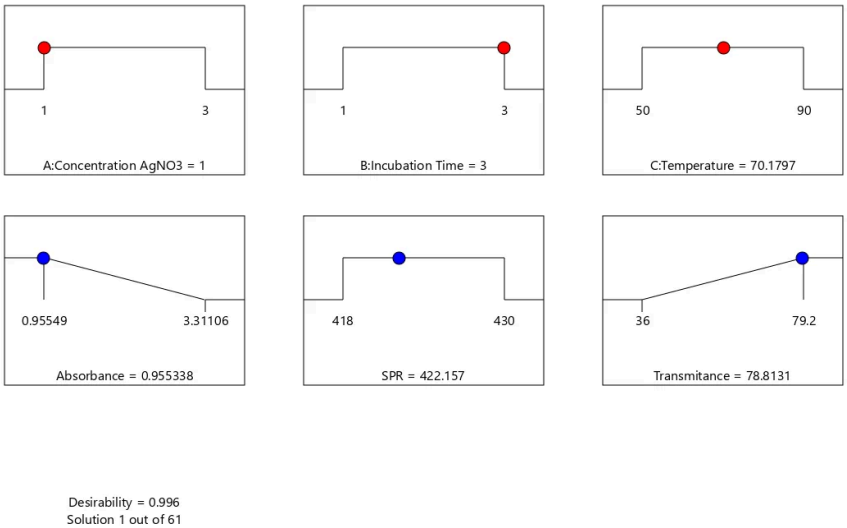

Figure 4. Design-Expert point prediction results identifying the optimal Ag-NP synthesis conditions based on maximum desirability.

values, confirming an adequate model fit. The effect of the independent variables on absorbance was described by a quadratic model, indicating that $AgNO_3$ concentration (A) had the most significant positive impact, with higher concentrations increasing absorbance (**Supplemental Equation 1 and Figure 1**).

A quadratic model well described the absorbance response. The model indicated that heating temperature (°C) exerted a significant positive effect on the SPR response, shifting the SPR peak toward longer wavelengths (**Supplemental Equation 2** and **Figure 2**).

The transmittance response was adequately described by a two-factor interaction (2FI) model. The negative coefficient of $AgNO_3$ concentration (A) indicated that increasing $AgNO_3$ concentration decreased transmittance due to enhanced nanoparticle formation and greater light absorption. The negative interaction between $AgNO_3$ concentration and incubation time (AB) further reduced transmittance, whereas heating temperature (C) exerted a positive effect under specific conditions (**Supplemental Equation 3 and Figure 3**). Overall, transmittance showed an inverse relationship with absorbance, as expected by the Beer–Lambert law.

The Design-Expert optimization identified the optimal conditions for Ag-NP synthesis as an $AgNO_3$ concentration of 1 mM, an incubation time of 3 h, and a temperature of approximately 70 °C, yielding a high desirability value of 0.996 (**Figure 4**). Under these conditions, the predicted responses were an absorbance of 0.955, an SPR peak at 422.16 nm, and a transmittance of 78.81%, confirming efficient silver nanoparticle formation with favorable optical properties. The experimental validation results showed good agreement with the predicted optimum responses, with all experimental values falling within the 95% confidence interval (CI) of the model predictions. The observed absorbance, SPR peak, and transmittance values

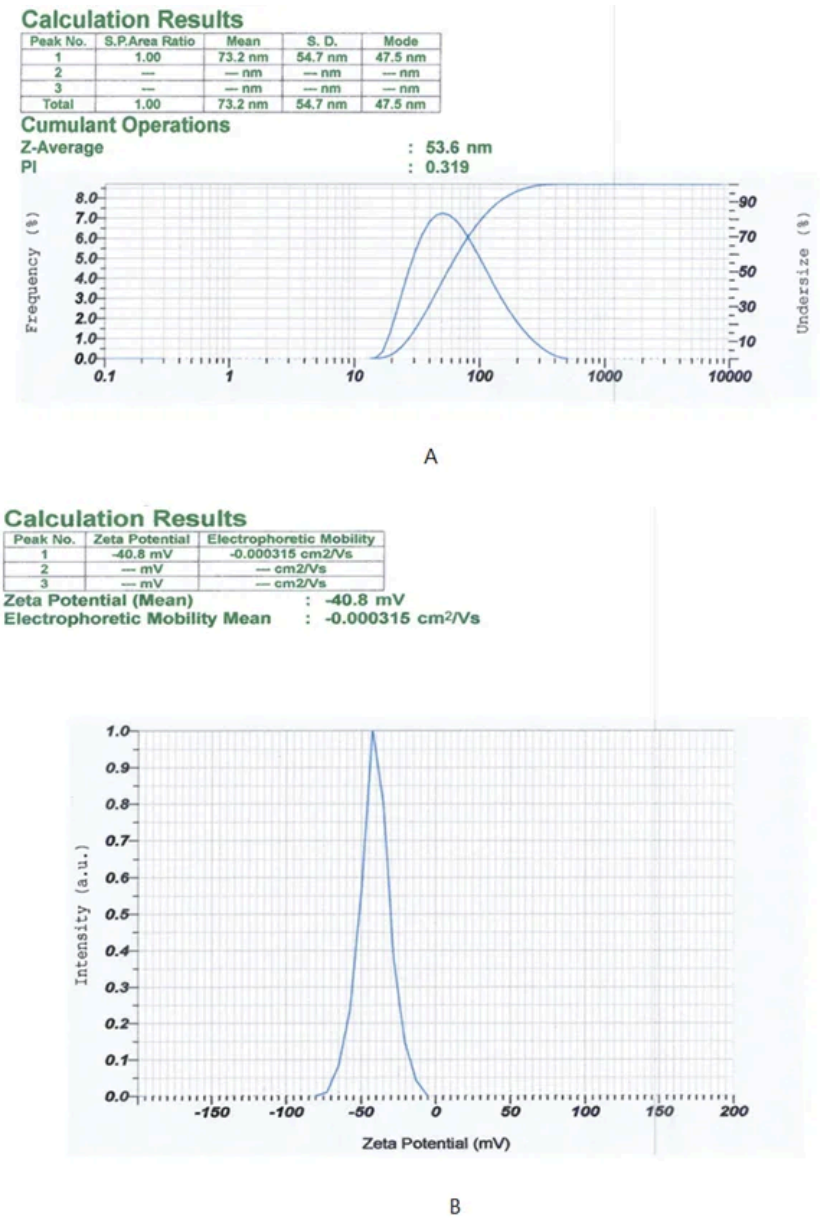

Figure 5. Particle size distribution and zeta potential of optimized silver nanoparticles in replication 3: (A) DLS analysis showing a Z-average particle size; (B) zeta potential distribution.

were comparable to the predicted results and remained within the characteristic range of silver nanoparticles. These findings confirm the adequacy and predictive reliability of the optimization model at a 95% confidence level.

Characterization of Optimized Silver Nanoparticles

The optimized silver nanoparticles were characterized for particle size, polydispersity index (PDI), and zeta potential using a dynamic light scattering (DLS) particle size analyzer. As shown in **Figure 5** and **Table 5**, the nanoparticles exhibited an average particle size of 53.6 ± 2.3 nm, indicating successful nanoscale formation. The PDI value (0.269 ± 0.058) reflected a narrow and homogeneous size distribution, while the zeta potential (−41.1 ± 0.7 mV) indicated high colloidal stability due to strong electrostatic repulsion. (4) Overall, these results confirm that the biosynthesized silver nanoparticles were stable, well-dispersed, and consistent with standard nanoparticle characteristics.

FTIR analysis was conducted to identify functional groups involved in the synthesis and stabilization of silver nanoparticles. *E. subumbrans* leaf extract spectrum exhibited a broad absorption band at 3311.68 cm^{-1}, corresponding to –OH group vibrations, typically associated with phenolic and flavonoid compounds (**Figure 6A**). Additionally, the band at 1634.71 cm^{-1} indicates the presence of aromatic C=C and/or conjugated C=O groups, which also act as reducing agents in nanoparticle synthesis. After the formation of AgNPs, a shift in the absorption band to 3266.78 cm^{-1} for the –OH group was observed, indicating interaction between hydroxyl groups and the nanoparticle surface. This shift suggests the involvement of bioactive compounds in the reduction of Ag^{+} to Ag^{0} and in its stabilization. Furthermore, the appearance of a new band at 2917.42 cm^{-1}, corresponding to C–H vibrations, indicates the contribution of organic compounds in the capping of the nanoparticles (25, 26). SEM images revealed irregularly shaped nanoparticles with relatively rough surfaces and a tendency toward agglomeration (**Figure 6B**), a common feature of plant-mediated green synthesis. The SEM images show nanoparticle agglomeration, which the drying process may influence during sample preparation. Solvent evaporation can induce capillary forces and particle clustering, leading to aggregation that may not reflect the true colloidal dispersion state of the nanoparticles (27, 28). XRD analysis exhibited distinct diffraction peaks corresponding to the (111), (200), (220), (311), and (222) planes (**Figure 6C**), confirming a face-centered cubic (FCC) crystalline structure consistent with standard silver nanoparticles (JCPDS No. 04-0783). The crystallite size of AgNPs, calculated from the (111), (200), (220), (311), and (222) peaks using the Scherrer equation, is 11.37 nm, confirming nanoscale crystalline silver consistent with green-synthesized AgNPs.

Antibacterial Activity Assay

The antibacterial activity of the optimized silver nanoparticle formulation against *Propionibacterium acnes* was evaluated using the disc diffusion method. The silver nanoparticles produced a mean inhibition zone diameter of 19.97 ± 0.83 mm, comparable to the positive control, Mediklin® Gel 1% (21.84 ± 1.67 mm), and higher than that of $AgNO_3$ solution (11.28 ± 5.96 mm) (**Table 6**). At the same time, the *E. subumbrans* leaf extract showed no inhibition zone. Statistical analysis revealed significant differences among treatments ($p < 0.001$), and Duncan's *post hoc* test placed the silver nanoparticles in the same subset as the positive control. These results indicate that silver nanoparticle formation significantly enhances antibacterial activity, likely due to nanoscale particle size and increased surface area that promote stronger interactions with bacterial cells (29, 30).

Conclusion

This study demonstrates the successful green synthesis of silver nanoparticles from *E. subumbrans* leaf extract under optimized conditions, yielding stable, bioactive AgNPs. The synthesized nanoparticles exhibited enhanced antibacterial activity against Propionibacterium acnes,

Table 5. Particle size distribution and zeta potential of optimized silver nanoparticles.

Replication	Particle size (nm)	PDI	Zeta potential (mV)
1	51.3	0.283	- 40.6
2	55.9	0.205	- 41.9
3	53.6	0.319	- 40.8
Avarege ±SD	53.6 ± 2.3	0.269 ± 0.058	- 41.1 ± 0.7

Table 6. Antibacterial activity of the optimized silver nanoparticles against Propionibacterium acnes expressed as inhibition zone diameter.

Specimen	Inhibition Zone Diameter (mm)			Mean ± SD
	Replicate 1	Replicate 2	Replicate 3	
Positive control (Mediklin® Gel 1%)	20.43	21.42	23.69	21.84 ± 1.67
Negative control ($AgNO_3$ solution)	14.56	14.90	4.41	11.28 ± 5.96
Leaf extract	0	0	0	0
Silver nanoparticles	19.66	20.92	19.34	19.97 ± 0.83

indicating their potential as alternative antimicrobial agents. However, this study is limited to preliminary antibacterial evaluation using the disc diffusion method. Further studies, including MIC/MBC determination, cytotoxicity assessment, and formulation development, are necessary to support their application, particularly in topical treatments such as acne therapy.

Abbreviations

E. subumbrans= *Erythrina subumbrans*; $AgNO_3$ = Silver Nitrate; AgNPs = Silver Nanoparticle; SEM = scanning electron microscopy; FTIR = Fourier transform infrared spectroscopy; XRD= X-ray diffraction; PSA= Particle Size Analyzer; PDI= Polydispersity index; SPR= surface plasmon resonance;

Declaration

Author Information

Indri Maharini
*Corresponding author
Department of Pharmaceutics, Faculty of Medicine and Health Sciences, Universitas Jambi, Jambi - 36361, Indonesia.
Contribution: Conceptualization, Funding acquisition, Methodology, Writing - Review & Editing.

Karen Putri Utami
Department of Pharmaceutics, Faculty of Medicine and Health Sciences, Universitas Jambi, Jambi - 36361, Indonesia.
Contribution: Data Curation.

Lilis Rachmawati
Department of Pharmaceutics, Faculty of Medicine and Health Sciences, Universitas Jambi, Jambi - 36361, Indonesia.
Contribution: Visualization.

Fitrianingsih Fitrianingsih
Department of Pharmaceutics, Faculty of Medicine and Health Sciences, Universitas Jambi, Jambi - 36361, Indonesia.
Contribution: Supervision, Writing - Review & Editing.

Puspa Dwi Pratiwi
Department of Pharmaceutics, Faculty of Medicine and Health Sciences, Universitas Jambi, Jambi - 36361, Indonesia.
Contribution: Formal analysis, Investigation, Validation.

Acknowledgment

The authors gratefully acknowledge the Directorate of Downstreaming and Partnerships, Directorate General of Research and Development, Ministry of Higher Education, Science, and Technology, Republic of Indonesia, for financial support and research facilitation under Contract No. 53/SPK/C.C4/PPK.DHK/VII/2025. The authors also thank all parties who contributed to the completion of this study.

Conflict of Interest

The authors declare no conflicting interest.

Data Availability

All data generated or analyzed during this study are included in this published article

Ethics Statement

Ethical approval was not required for this study.

Funding Information

This work was supported by the Directorate of Downstreaming and Partnerships, Directorate General of Research and Development, Ministry of Higher Education, Science, and Technology, Republic of Indonesia, under Grant Number 53/SPK/C.C4/PPK.DHK/VII/2025.

Supplementary Material

This article contains supplementary material, including **Supplemental Equations 1**, **2**, and **3**, which are available online.

References

1. Susilawati E, Levita J, Susilawati Y, Sumiwi S. *Erythrina subumbrans* (Hassk) Merr. (Fabaceae) Inhibits Insulin Resistance in the Adipose Tissue of High Fructose-Induced Wistar Rats. Dddt. 2024;Volume 18:3825-3839. doi: https://doi.org/10.2147/dddt.s472660

2. Rangkuti SN, Aprilliani A, Sulestari F. Farmagazine. 2023; 10 (2): 17–27.

3. Ayu Putu Chika Iswari Anjani S, Ratna Sari Dewi K, Gede Bayu Surya Ekayana I, Chandra Yowani S. Aktivitas Lotion Tabir Surya Ekstrak Daun Dadap Serep (*Erythrina subumbrans*) dan Daun Kelor (*Moringa oleifera* L.) Secara In-Vitro. Jurnal Global Ilmiah. 2025;2(4):1-10. doi: https://doi.org/10.55324/jgi.v2i4.179

4. Maharini I, Fitrianingsih F, Utami DT. Green synthesis nanoperak menggunakan ekstrak batang dadap serep (*Erythrina Subumbrans* (Hassk.) Merr). Jps. 2023;6(5):255-259. doi: https://doi.org/10.36490/journal-jps.com.v6i5-si.410

5. Phukhatmuen P, Meesakul P, Suthiphasilp V, Charoensup R, Maneerat T, Cheenpracha S, et al. Antidiabetic and antimicrobial flavonoids from the twigs and roots of *Erythrina subumbrans* (Hassk.) Merr. Heliyon. 2021;7(4):e06904. doi: https://doi.org/10.1016/j.heliyon.2021.e06904

6. Panjaitan KN, Syamsurizal S, Maharini I, Putra DOY, Septiana P. Optimasi dan Uji Antibakteri Nanopartikel Perak dengan Bioreduktor Ekstrak Batang Anggrek Merpati (*Dendrobium crumenatum* Sw.). sinteza. 2025;5(1):18-31. doi: https://doi.org/10.29408/sinteza.v5i1.29574

7. Maharini I, Havizur R, Utami DT. The effect of concentration liquid extract gaharu (*Aquilaria malaccensis*) leaves on green synthesis nanosilver. In: Asian Federation for Pharmaceutical Sciences (AFPS); 2019.

8. Bemis R, Deswardani F, Heriyanti H, Puspitasari RD, Azizah N. Green Synthesis of Silver Nanoparticles Using *Areca catechu* L Peel Bioreductor as an Antibacterial

Escherichia coli and *Staphylococcus aureus*. Ind. J. Chem. Anal. 2023;6(2):176-186. doi: https://doi.org/10.20885/ijca.vol6.iss2.art9

9. Fajri N, Putri LFA, Prasetio MR, Azizah N, Pratama Y, Susanto NCA. Potensi Batang Pisang (*Musa paradisiaca* l) sebagai bioreduktor dalam Green Sintesis Ag nanopartikel. Jps. 2022;24(1):33. doi: https://doi.org/10.56064/jps.v24i1.668

10. Zulaicha AS, Saputra IS, Sari IP, Ghifari MA, Yulizar Y, Permana YN, et al. Green Synthesis Nanopartikel Perak (AgNPs) Menggunakan Bioreduktor Alami Ekstrak Daun Ilalang (Imperata cylindrica L). rjna. 2021;1(1):11-19. doi: https://doi.org/10.33369/rjna.v1i1.15588

11. Joseph T, Kar Mahapatra D, Esmaeili A, Piszczyk Ł, Hasanin M, Kattali M, et al. Nanoparticles: Taking a Unique Position in Medicine. Nanomaterials. 2023;13(3):574. doi: https://doi.org/10.3390/nano13030574

12. Duffy LL, Osmond-McLeod MJ, Judy J, King T. Investigation into the antibacterial activity of silver, zinc oxide and copper oxide nanoparticles against poultry-relevant isolates of Salmonella and Campylobacter. Food Control. 2018;92:293-300. doi: https://doi.org/10.1016/j.foodcont.2018.05.008

13. Al-Momani H, Massadeh MI, Almasri M, Al Balawi D, Aolymat I, Hamed S, et al. Anti-Bacterial Activity of Green Synthesised Silver and Zinc Oxide Nanoparticles against *Propionibacterium acnes*. Pharmaceuticals. 2024;17(2):255. doi: https://doi.org/10.3390/ph17020255

14. Joshi V, Bachhar V, Mishra SS, Shukla RK, Duseja M. Hexagonal ZnO nanoparticles synthesised using methanolic extract of *Piper chaba* aerial parts for catalytic oxidation of morin, 4-nitrophenol reduction, antioxidant and antibacterial applications. Journal of Molecular Structure. 2025;1348:143550. doi: https://doi.org/10.1016/j.molstruc.2025.143550

15. Bachhar V, Joshi V, Pant P, Duseja M, Chitme H, Sharma N. Green synthesis of TiO2/Ag/Cu2O nanoparticles: Antioxidant potential and in-vitro/in-vivo antidiabetic activity in STZ-induced diabetic albino mice. Inorganic Chemistry Communications. 2026;183:115900. doi: https://doi.org/10.1016/j.inoche.2025.115900

16. Bachhar V, Joshi V, Singh A, Mir MA, Bhardwaj A. Antibacterial, antioxidant, and antidiabetic activities of TiO_2 nanoparticles synthesized from Euphorbia hirta. 2025; 14 (1): 1–13.

17. Tabasum H, Bhat BA, Sheikh BA, Mehta VN, Rohit JV. Emerging perspectives of plant-derived nanoparticles as effective antimicrobial agents. Inorganic Chemistry Communications. 2022;145:110015. doi: https://doi.org/10.1016/j.inoche.2022.110015

18. Kailasa SK, Park TJ, Rohit JV, Koduru JR. Antimicrobial activity of silver nanoparticles. Elsevier; 2019. doi: https://doi.org/10.1016/b978-0-12-816504-1.00009-0

19. Mushtaq M, Rohit JV. Enhancing the medicinal potency of Colchicum luteum by forming biogenic silver nanoparticles: Antimicrobial, anticancer and antioxidant evaluation. Microbial Pathogenesis. 2026;210:108181. doi: https://doi.org/10.1016/j.micpath.2025.108181

20. Reshi MA, Ara T, Rohit JV. Biogenic metal nanoparticles based visual sensor for the monitoring of environmental pollutants. Microchemical Journal. 2025;219:115839. doi: https://doi.org/10.1016/j.microc.2025.115839

21. Eker F, Akdaşçi E, Duman H, Bechelany M, Karav S. Green Synthesis of Silver Nanoparticles Using Plant Extracts: A Comprehensive Review of Physicochemical Properties and Multifunctional Applications. Ijms. 2025;26(13):6222. doi: https://doi.org/10.3390/ijms26136222

22. Vanlalveni C, Lallianrawna S, Biswas A, Selvaraj M, Changmai B, Rokhum SL. Green synthesis of silver nanoparticles using plant extracts and their antimicrobial activities: a review of recent literature. RSC Adv. 2021;11(5):2804-2837. doi: https://doi.org/10.1039/d0ra09941d

23. Almatroudi A. Silver nanoparticles: synthesis, characterisation and biomedical applications. Open Life Sciences. 2020;15(1):819-839. doi: https://doi.org/10.1515/biol-2020-0094

24. Siregar NC, Yanti DD, Ashari A, Aji A. Application of silver nanoparticles synthesised using Moringa leaf extract for detection of mercury ions. Stannum J Sains Terap Kim. 2025; 7 (1): 37–45.

25. Esther Arland S, Kumar J. Green and chemical syntheses of silver nanoparticles: Comparative and comprehensive study on characterization, therapeutic potential, and cytotoxicity. European Journal of Medicinal Chemistry Reports. 2024;11:100168. doi: https://doi.org/10.1016/j.ejmcr.2024.100168

26. Satria D, Siregar NA, Waruwu SB, Putra EDL, Sinaga SM, Septama AW, et al. Eco-friendly one-pot synthesis of silver nanoparticles via microwave irradiation using *Artocarpus camansi* extract: Characterization, antioxidant, and antibacterial applications. J King Saud Univ Sci. 2026;38:10112025. doi: https://doi.org/10.25259/jksus_1011_2025

27. Furxhi I, Faccani L, Zanoni I, Brigliadori A, Vespignani M, Costa AL. Design rules applied to silver nanoparticles synthesis: A practical example of machine learning application. Computational and Structural Biotechnology Journal. 2024;25:20-33. doi: https://doi.org/10.1016/j.csbj.2024.02.010

28. Kumarasamy RV, Natarajan PM, Mathivanan I, Balasubramaniam M, Sn S, Prabhu D, et al. Sustainable biogenic synthesis of silver nanoparticles for oral cancer: a comprehensive review. Front. Nanotechnol. 2026;7. doi: https://doi.org/10.3389/fnano.2025.1648900

29. Nalawati AN, Suyatma NE, Wardhana DI. Sintesis

Nanopartikel Perak (NPAg) dengan Bioreduktor Ekstrak Biji Jarak Pagar dan Kajian Aktivitas Antibakterinya. jtip. 2021;32(1):98-106. doi: https://doi.org/10.6066/jtip.2021.32.2.98

30. Saini P, Mushtaq M, Sofi TA, Anjum S, Bhat BA, Rohit JV. Sustainable management of plant fungus using nanobiopesticide of Delphinium cashmirianum derived bio silver nanoparticles. Sustainable Chemistry One World. 2026;9:100174. doi: https://doi.org/10.1016/j.scowo.2025.100174

Additional Information

How to Cite

APA 7th Edition: Maharini, I., Utami, K. P., Rachmawati, L., Fitrianingsih, F. & Pratiwi, P. D. (2026). Green-Synthesized Silver Nanoparticles Using Erythrina subumbrans Leaf Extract: Optimization and Antibacterial Activity. Sciences of Pharmacy, 5(2), 112-122. https://doi.org/10.58920/sciphar0502580

Vancouver: Maharini I, Utami KP, Rachmawati L, Fitrianingsih F, Pratiwi PD. Green-Synthesized Silver Nanoparticles Using Erythrina subumbrans Leaf Extract: Optimization and Antibacterial Activity. Sciences of Pharmacy. 2026;5(2):112-122. https://doi.org/10.58920/sciphar0502580

Harvard: Maharini, I., Utami, K. P., Rachmawati, L., Fitrianingsih, F. & Pratiwi, P. D. (2026) 'Green-Synthesized Silver Nanoparticles Using Erythrina subumbrans Leaf Extract: Optimization and Antibacterial Activity', Sciences of Pharmacy, 5(2), pp. 112-122. doi: 10.58920/sciphar0502580

Publisher Note

All claims expressed in this article are solely those of the authors and do not necessarily reflect the views of the publisher, the editors, or the reviewers. Any product that may be evaluated in this article, or claim made by its manufacturer, is not guaranteed or endorsed by the publisher. The publisher remains neutral with regard to jurisdictional claims in published maps and institutional affiliations.

Open Access

This article is licensed under a Creative Commons Attribution 4.0 International License. You may share and adapt the material with proper credit to the original author(s) and source, include a link to the license, and indicate if changes were made.